

Universal quantum reservoir computing

Sanjib Ghosh,^{1,*} Tanjung Krisnanda,¹ Tomasz Paterek,^{1,2,3} and Timothy C. H. Liew^{1,2,†}

¹*School of Physical and Mathematical Sciences,*

Nanyang Technological University 637371, Singapore

²*MajuLab, International Joint Research Unit UMI 3654,*

CNRS, Université Côte d'Azur, Sorbonne Université,

National University of Singapore, Nanyang Technological University, Singapore

³*Institute of Theoretical Physics and Astrophysics,*

Faculty of Mathematics, Physics and Informatics,

University of Gdańsk, 80-308 Gdańsk, Poland

We show that quantum reservoir neural networks offer an alternative paradigm for universal quantum computing. In this framework, a dynamical random quantum network, called the quantum reservoir, is used as a quantum processor for performing operations on computational qubits. We show various quantum operations including a universal set of quantum gates, which can be obtained with a single quantum reservoir network with different tunnelling amplitudes between the reservoir and the qubits. The same platform can also implement non-unitary quantum gates, which are useful to simulate open quantum systems with tuneable parameters.

In the era of big data and machine learning, neuromorphic computing is rapidly emerging as an alternative platform for computation and data processing. While conventional computers rely on predetermined algorithms for performing tasks, neuromorphic computers use artificial neural networks, which are flexible and can learn from example in analogy to a biological brain. Their resilience allows them to be versatile in applications and adaptive to practical situations. For instance, neural networks are used across disciplines for a multitude of tasks [1–7], and are capable of extracting features from noisy [8, 9] or incomplete data [10, 11], and perturbed systems [12].

An artificial neural network is a system of interconnected nonlinear nodes capable of modelling complex mapping between input and output data. A given map is formed by carefully adjusting the connection weights between the nodes during a training procedure.

While neural networks have been used for various applications, most of them are in the form of softwares implemented in conventional computers. However, hardware realizations are highly sought for exploiting the added efficiency in overcoming the so-called von Neumann bottleneck inherent in neural networks. A major challenge in hardware implementations is controlling the large number of connections between the nodes in conventional neural network architectures [13]. Reservoir computing is an alternative architecture where the connections are taken fixed and random [14], thus avoiding the overhead of controlling a large number of connections, while keeping its wide range of applications [15, 16]. Here, the fixed random network is known as the reservoir. As it is easier to engineer a fixed and random network than a well controlled one, reservoir computing is emerging as one of most successfully implemented neural networks in a variety of physical systems [17–19]. However, most of them are working in the classical domain aiming to boost classical information processing (even using quantum reservoirs [20]). Recently, the idea of reservoir computing was brought to the quantum world for quantum information processing [21]. While some of these examples are capable of performing certain quantum information processing tasks, they are incapable of universal quantum computing.

In quantum computing, one of the most commonly used architectures is the quantum circuit model where an arbitrary quantum operation is decomposed with elementary quantum operations known as quantum gates [22]. While quantum computing has the promise to change the course of future computing, its realization requires precise engineering [23], which has led to the developments of quantum computers with only limited number of qubits so far [24, 25], while the actual number required for meaningful applications is orders of magnitude higher [26]. Currently, most hardware realizes quantum operations by applying several quantum gates in sequence. Although any quantum operation can be in principle obtained by applying gate combinations from a small set of universal quantum gates, long gate sequences require long operation time and lead to large errors. Alternatively, many frequently used elementary quantum operations can be obtained directly instead of obtaining them as combinations of a single set of universal gates. However, realising different types of operations has required different types of interaction between the qubits, which needs even more complex engineering limiting their scalability.

Here, we consider the reservoir computing framework as a basis for universal quantum computing. In reservoir computing, the reservoir is taken as a randomly connected network,

which needs no optimisation itself and thus requires no precise engineering. Moreover, here we consider the connection between the nodes as basic quantum tunnelling as opposed to different types of interactions needed to achieve different quantum gates for conventional approaches. The only optimisation needed is in a control layer of connections (tunnelling amplitudes) between the qubits and the quantum reservoir, as described in Fig. 1. As opposed to conventional quantum computers, here the qubits do not interact with each other directly and are only connected via the quantum reservoir through simple quantum tunnelling. We show that a single quantum reservoir can induce a wide variety of quantum operations on the qubits while we only control the tunnelling amplitudes to the reservoir. Moreover, we show that our scheme can directly induce non-unitary quantum operations, which can be helpful to simulate open quantum systems.

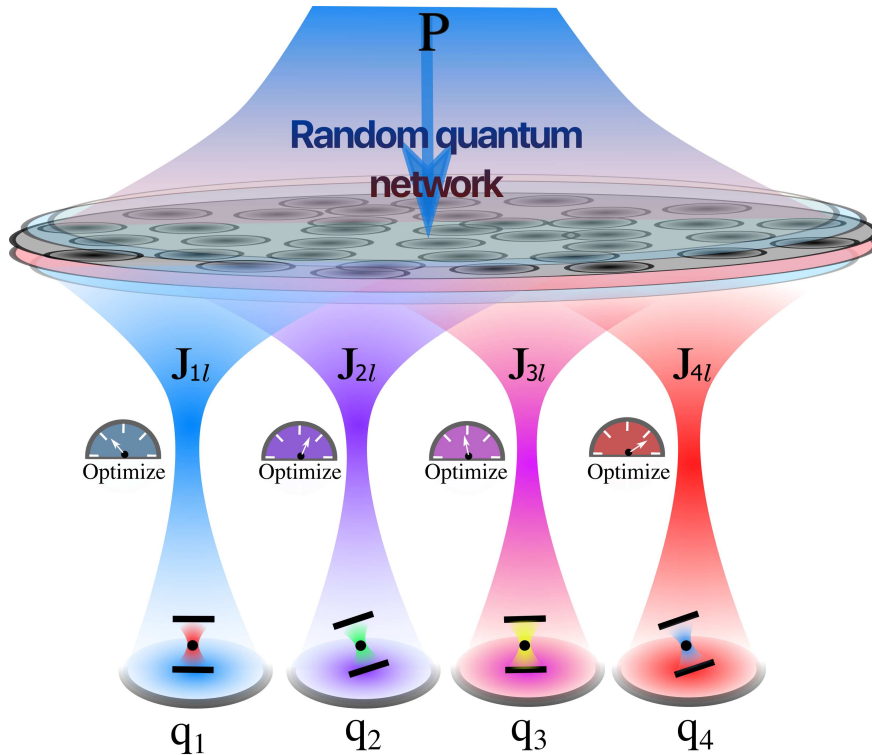


FIG. 1: The scheme for universal quantum computing based on a quantum reservoir neural network. In this framework, the network of randomly connected nodes driven with coherent excitation P is the so-called quantum reservoir. The qubits on which computation is performed are denoted by q_k . Quantum operations on qubits q_k are performed by coupling them through the reservoir. J_{kl} represent a control layer of tunnelling amplitudes connecting the qubits to the quantum network.

The model:– Our considered scheme is described in Fig. 1, where a quantum reservoir network is formed with a 2D lattice of fermions, which are interconnected via quantum tunnelling with random amplitudes and are excited with a classical field. The Fermi-Hubbard Hamiltonian representing the quantum reservoir network is given by,

$$\hat{H}_R = \sum_l E_l \hat{a}_l^\dagger \hat{a}_l + \sum_{\langle ll' \rangle} K_{ll'} (\hat{a}_l^\dagger \hat{a}_{l'} + \hat{a}_{l'}^\dagger \hat{a}_l) + \sum_l (P^* \hat{a}_l + P \hat{a}_l^\dagger), \quad (1)$$

where E_l and $K_{ll'}$ are site-dependent energies and nearest-neighbour hopping amplitudes, uniformly distributed in the intervals $[\pm E_0]$ and $[\pm K_0]$, respectively. P is the amplitude of a uniform classical optical excitation (e.g., a laser).

This fermionic network interacts with a set of qubits to realize the universal quantum processor. We consider that the qubits are independent and are connected to the quantum reservoir through quantum tunnelling with the amplitudes J_{kl} between the qubit q_k and the reservoir site l , such that the whole system is described by the Hamiltonian:

$$\hat{H} = \hat{H}_R + \sum_{kl} \left(J_{kl}^* \hat{\sigma}_k^+ \hat{a}_l + J_{kl} \hat{a}_l^\dagger \hat{\sigma}_k^- \right), \quad (2)$$

where $\hat{\sigma}_k^\pm = \hat{\sigma}_k^x \pm i \hat{\sigma}_k^y$ with $\hat{\sigma}_k^x$ and $\hat{\sigma}_k^y$ being the Pauli-X and Y operators for the qubit q_k . Note that the qubits do not directly interact with each other, but only with the quantum reservoir through quantum tunnelling. Here our proposition is to induce universal quantum operations on the qubits q_k only with suitable tunnelling amplitudes J_{kl} . The appropriate J_{kl} are obtained by training. In training, we sample a set of pure input states for the qubits and compute fidelity of the states resulting from the reservoir computing to the ideal states obtained by applying a desired quantum operation. The optimization is performed using a hybrid genetic Nelder-Mead algorithm to set the tunnelling amplitudes J_{kl} (more details are given in the Appendix). In practice, this procedure requires access to a set of ideal input-output state pairs, which can either be calculated theoretically or taken as a resource in an experimental setup. We allow J_{kl} to be complex, for generality, however this is not strictly necessary for our scheme. Once J_{kl} are optimized, the fidelity is retested with a different sample of input states.

The Fermi-Hubbard model represented by the Hamiltonian \hat{H} has efficiently been implemented using cold atoms in optical lattices [27–29] and is expected to be accessible

in nonlinear cavity arrays [30, 31], depending on the strongly interacting photon regime. Substantial progress has been made toward reaching this regime using a variety of systems, including Rydberg atoms in high quality factor cavities [32], photonic crystal structures [33], superconducting circuits [34], exciton-polaritons [35], and trion-polaritons [36, 37]. A variety of physical implementations of coupling of quantum emitters to waveguides [38] or resonators [39] have also been considered, where lattices of superconducting qubits [40] have been particularly successful. These classes of systems are typically described by the Jaynes-Cummings-Hubbard model [41, 42] where bosonic cavity modes are used to couple separated fermionic modes. In the limit that the cavity mode detuning is larger than the energy exchange between the bosons and fermions, the bosonic modes can be eliminated, returning to an effective Fermi-Hubbard model [43].

Quantum operations:— Here we describe the protocol for inducing quantum operations on the qubits. An operation begins at time $t = 0$ with the initialization of qubits. We sample the initial states $|\varphi_{\text{in}}\rangle$ uniformly at random. We consider that the quantum reservoir network starts with the vacuum state $|\text{vac}\rangle_R$. The evolution of the whole system is then allowed up to a time $t = \tau$ under the classical coherent excitation represented by P and the tunnelling amplitudes J_{kl} obtained from training. We imagine that the evolution is enabled by pulses of duration τ controlling the excitation and the tunnelling amplitudes J_{kl} . The evolution of the whole system is given by the unitary operation $\hat{U} = \exp[-i\hat{H}\tau/\hbar]$. The final state of the combined system is thus given by $|\Psi_{\text{out}}\rangle = \hat{U} |\varphi_{\text{in}}\rangle \otimes |\text{vac}\rangle_R$. Although the global operation \hat{U} is unitary, the induced operation on the qubits is not necessarily unitary. This follows from the fact that during the evolution, quantum information can flow out from the qubits into the reservoir. The final state of the qubits is thus most generally represented by the density matrix $\rho_q = \text{Tr}_R[|\Psi_{\text{out}}\rangle\langle\Psi_{\text{out}}|]$ where $\text{Tr}_R[\dots]$ represents the partial trace that traces out the quantum reservoir. For each initial state we compute the fidelity given by the overlap of the ideal final quantum state $|\varphi_{\text{ideal}}\rangle = \hat{u}_q|\varphi_{\text{in}}\rangle$ and the obtained state ρ_q :

$$F = \langle\varphi_{\text{ideal}}|\rho_q|\varphi_{\text{ideal}}\rangle \quad (3)$$

where \hat{u}_q is the desired quantum operation for the qubits. We plot fidelity histograms to show that the realised gates are almost perfect for any input state.

For universal quantum computing, realizing a controlled-NOT (cNOT) gate together with certain single qubit gates is sufficient. However, here we show that the same quantum reser-

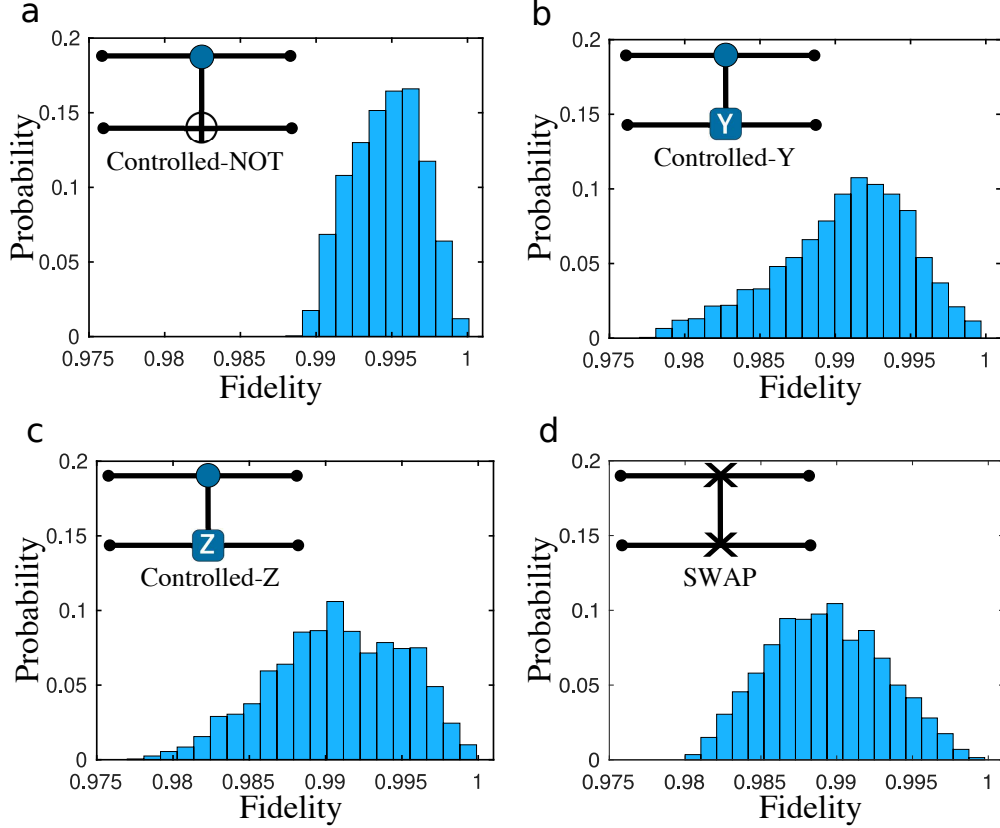


FIG. 2: Two-qubit gates and their fidelity distributions. **a**, **b**, **c**, and **d** are the fidelity distributions of the realised operations with quantum reservoir networks for cNOT, cY, cZ and SWAP as shown in the insets. Here we consider 6 fermions for the quantum reservoir. The fidelity distributions are obtained over 2000 uniformly at random generated states. The average fidelity for all gates are larger than 0.99, which is a standard parameter in process tomography. The considered parameters are presented in Table I in the Appendix.

voir neural network can realize a range of different two-qubit gates, e.g., cNOT, controlled-Y (cY), controlled-Z (cZ) and SWAP (see Fig. 2). A specific gate operation is induced with well chosen tunnelling amplitudes J_{kl} and the pulse duration τ . In Fig. 3, we also demonstrate that high fidelity single-qubit gates are realized with a reservoir network consisting of only one node. These quantum gates and the two-qubit gates shown in Fig. 2 can perform any quantum operation.

Discussion:– We have presented a platform for universal quantum computing where an underlying set of quantum nodes connects computing qubits and a learning algorithm is used to adapt the system to a particular quantum operation. Several previous works

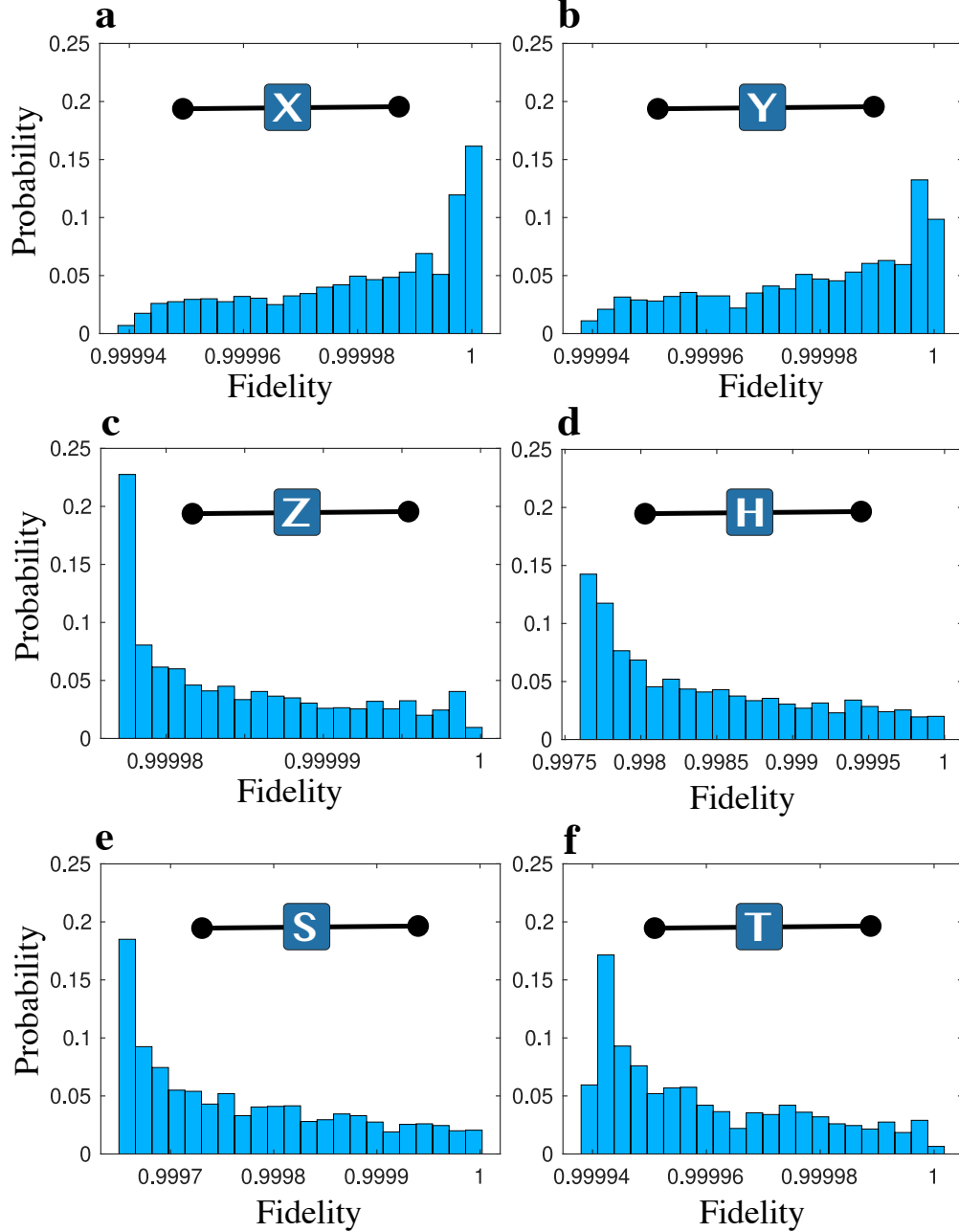


FIG. 3: Fidelities of the single-qubit gates. We show the fidelity distributions for different single-qubit gates over 2000 uniformly at random generated states. **a** to **f** show the fidelity distributions for Pauli-X, Y, Z, Hadamard, phase and $\pi/8$ gates. Here we find that a single fermionic node as the quantum reservoir is sufficient to induce the gates required for the computational universality. The average fidelity for all the single qubit gates are larger than 0.9984. The considered parameters are listed in Table II in the Appendix.

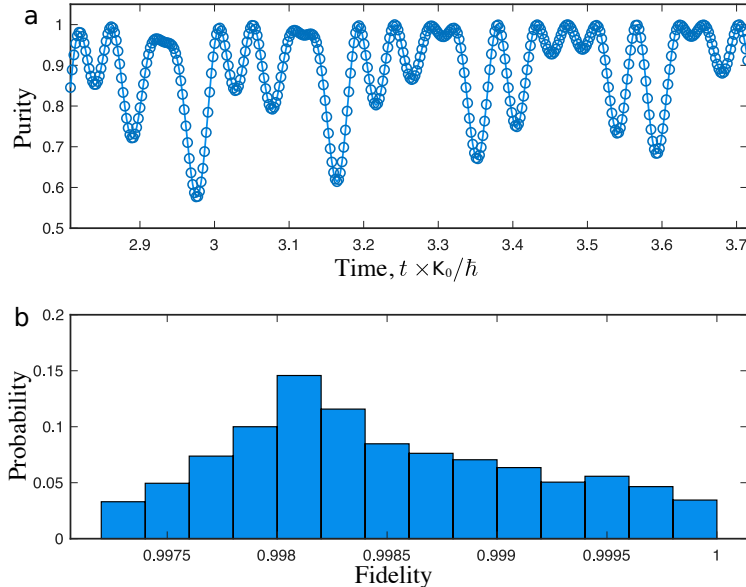


FIG. 4: A quantum reservoir can induce nonunitary operation. **a**, Purity of a qubit undergoing a quantum reservoir operation as a function of the operation time. **b**, Distribution of fidelity of a qubit evolving under a Markovian process. We consider a decay strength γ and a propagation time $t = 0.5\hbar/\gamma$ for the Markovian process. Here, we considered a single fermionic node for the reservoir and 2000 uniformly-at-random distributed initial states.

have considered how quantum neural networks can enhance the efficiency of solving classical tasks [20, 44, 45], while others have considered the use of assumed quantum computers [46–49] and quantum annealers [50] in neuromorphic architectures. In contrast, here we imagine a neuromorphic architecture that can allow a set of quantum nodes to realize universal quantum computation. The learning of quantum operations from quantum networks has been considered before, based on nonlocal spin coupling [51] and adiabatic pulse control [52]. The advantage of the reservoir network architecture introduced here is that only quantum tunnelling is considered for network connections, which is readily accessible in many systems (e.g. photonics, polaritons, cold atoms, and trapped ions), and, that only a small subset of total network connection weights need to be controlled. We note that a very simple learning algorithm in the optimization of the tunnelling amplitudes was used. The application of more advanced evolutionary algorithms in quantum control would likely lead to improved results for our system [53].

In general, the operations induced by the quantum reservoir on the qubits are nonunitary

in nature. The signature of the nonunitary nature of the operation can be observed in the purity of the qubits. In Fig. 4 **a**, we show the purity of a qubit undergoing a quantum reservoir operation as a function of operation time. We find that the purity of the qubit oscillates and reaches 1 only at certain times. The effective operation on the qubit is thus unitary only at those times. The system can therefore implement non-unitary gates. For a demonstration we consider a Markovian dynamics for the qubit given by the master equation: $\hbar\dot{\rho} = (\gamma/2)(2\sigma^-\rho\sigma^+ - \sigma^+\sigma^-\rho - \rho\sigma^+\sigma^-)$. Using the quantum reservoir, we obtain a non-unitary quantum operation equivalent to the same induced by the master equation of the qubit. In Fig. 4 **b**, we show the fidelity between the quantum states obtained from quantum reservoir processing and from solving the quantum master equation.

APPENDIX

Training

One of the main features of neural network frameworks is that they learn from examples without being told the specific rules of the task. Here we take advantage of this powerful feature and use it for realizing various quantum operations by training the quantum reservoir network. While in conventional approaches, different quantum gate operations require realizing different types of interactions between the qubits, here, the same quantum network is used to obtain different operations. Given a quantum operation \hat{u}_q , that we want to realize, we consider a set of example quantum states $|\varphi_{\text{in}}^{(j)}\rangle$ for the qubits for training. For each example quantum state $|\varphi_{\text{in}}^{(j)}\rangle$, we calculate the fidelity F_j given by Eq. 3. We numerically maximize the average fidelity

$$\bar{F} = \frac{1}{N} \sum_{j=1}^N F_j \quad (4)$$

with optimal choice of tunnelling amplitudes J_{kl} , where N is the number of quantum states in the training set. We empirically find that for two-qubit gate operation 10 randomly generated quantum states are sufficient for training.

Training of the quantum neural network is an optimization process. The average fidelity $\bar{F}(J_{kl})$ is a nonlinear function of the tunnelling amplitudes J_{kl} . For a small number of parameters J_{kl} , a deterministic method such as the Nelder-Mead simplex algorithm is sufficient

Gate	E_0/K_0	P/K_0	$\tau K_0/\hbar$
cNOT	1	400	0.15
cY	1	400	0.135
cZ	1	154	0.15
SWAP	2	5.5	0.2

TABLE I: Parameters considered to obtain two-qubit gates. These gates are obtained with a quantum reservoir of 6 sites.

to achieve the optimum condition. However, for large numbers of J_{kl} , we use a stochastic genetic algorithm to find the optimum condition starting from a set of initial guesses, which approach the optimum point in a random process.

Genetic algorithms are inspired by the biological evolution based on natural selection. The process starts with a random set of populations that goes through a natural selection procedure based on a fitness criterion. The fittest individuals reproduce the next generation of populations through a cross breeding procedure. Random mutation in the new generation ensures diversity among the populations.

Here, J_{kl} with all k and l represent one individual in a genetic algorithm. We define a population with a set of M such individuals J_{kl}^m where $m = 1, 2 \dots M$. We start with a random choice of population. The fitness criterion is defined through calculating the average fidelity $\bar{F}(J_{kl}^m)$ for an individual m .

The next generation of population is reproduced by the two individuals with largest average fidelities, keeping the total population size fixed to M . The next generation J_{kl}^m is born with the cross breeding rule:

$$J_{kl}^m = (J_{kl}^p + J_{kl}^q)/2 + \delta f_{\text{ran}} \quad (5)$$

where δ and f_{ran} represent a mutation rate and a Gaussian random number, respectively. The process of natural selection is then repeated for the new generation until the optimum condition is found.

Parameters:– The considered parameters for obtaining the quantum gate operations are noted in tables I and II.

Gate	E_0/K_0	P/K_0	$\tau K_0/\hbar$	Gate	E_0/K_0	P/K_0	$\tau K_0/\hbar$
X	1	60	2.032	H	1	4.96	1
Y	1	60	11	S	1	0.1	2.02
Z	1	0.1	4.14	T	1	0.1	3.11

TABLE II: Parameters considered to obtain single-qubit quantum gates. The single-qubit gates are obtained with a single reservoir site.

One-qubit gates

The setup:— Here we consider a special case where one input qubit interacts with a one-site reservoir (a fermion). The reservoir has an onsite energy E_1 , a coherent driving (pump) P , and negligible decay. The dynamics of the whole system is unitary, where the Hamiltonian is written as

$$H = E_1 \hat{a}_1^\dagger \hat{a}_1 + P \hat{a}_1^\dagger + P^* \hat{a}_1 + J_{11} (\hat{\sigma}_1^+ \hat{a}_1 + \hat{a}_1^\dagger \hat{\sigma}_1^-), \quad (6)$$

with J_{11} being the strength of the coupling term. Note that we have used $\hat{\sigma}_1^-$ (\hat{a}_1) as the annihilation operator of the input qubit (the reservoir site). Below we will present the working parameters for the dynamics of this system such that the evolution of the input qubit implements the X, Y, and Z gates given by the Pauli operators

$$\hat{\sigma}^x = \begin{pmatrix} 0 & 1 \\ 1 & 0 \end{pmatrix}, \quad \hat{\sigma}^y = \begin{pmatrix} 0 & -i \\ i & 0 \end{pmatrix}, \quad \hat{\sigma}^z = \begin{pmatrix} 1 & 0 \\ 0 & -1 \end{pmatrix}, \quad (7)$$

respectively. We will present two regimes, namely the low and high reservoir energy limit, in which one can implement the one-qubit gates on the input qubit.

Low energy limit ($E_1 \ll |P|, J_{11}$):— First of all, note that the most important component in the system is given by the hopping interaction between the input qubit and the reservoir. In particular, if one were to consider this term alone, the eigenstates and eigenvalues are given by $\{|00\rangle, |11\rangle, |\psi_-\rangle, |\psi_+\rangle\}$ and $\{0, 0, -J_{11}, J_{11}\}$, respectively. We have used the Bell-state notation $|\psi_\pm\rangle = (|01\rangle \pm |10\rangle)/\sqrt{2}$. Therefore, one can see that, in the case of $E_1 = |P| = 0$, the evolution of the system follows $\hat{U}(t) = |00\rangle\langle 00| + |11\rangle\langle 11| + \exp(iJ_{11}t/\hbar)|\psi_-\rangle\langle\psi_-| + \exp(-iJ_{11}t/\hbar)|\psi_+\rangle\langle\psi_+|$, which, at $J_{11}\tau/\hbar = \pi + 2\pi n$, reduces to

$$\hat{U}(\tau) = \hat{\sigma}_q^z \otimes \hat{\sigma}_r^z, \quad (8)$$

where the subscript q (r) denotes the input qubit (the reservoir). This evolution executes the Z gate on the input qubit.

For the implementation of the X and Y gates, let us first note that if we consider only the pumping term of the reservoir, one can either have $H \propto \hat{\sigma}_r^x$ when the pump P is real or $H \propto \hat{\sigma}_r^y$ when the pump has a phase, in particular, $P = |P| \exp(\pm i\pi/2)$. This allows the application of either the X or Y gate on the state of the reservoir at $|P|\tau/\hbar = \pi/2 + \pi n$. In order to implement the gates on the state of the input qubit, let us consider the interaction J_{11} in addition to the reservoir pumping term, and also assume the strength $|P| \gg J_{11}$. In this limit, one can confirm that the evolution operator of the system, at time $J_{11}\tau/\hbar = \pi + 2\pi n$, where $n = 0, 1, 2, \dots$, is given by

$$\hat{U}(\tau) = e^{-i(\pi/2+\pi n)} \hat{\sigma}_q^x \otimes \hat{\sigma}_r^x, \quad (9)$$

$$\hat{U}(\tau) = e^{-i(\pi/2+\pi n)} \hat{\sigma}_q^y \otimes \hat{\sigma}_r^y, \quad (10)$$

if P is real and $P = |P| \exp(\pm i\pi/2)$ is imaginary, respectively. These evolution operators realise the X (Eq. 9) and Y (Eq. 10) gates. Furthermore, the addition of the onsite energy, with $E_1 \ll |P|$, does not change the conclusion as it simply adds an overall phase to the gate.

In order to have control over the application of the gates above, one can consider a system in a regime where $|P| \gg J_{11} \gg E_1$. It is apparent that in this way, one can control (to some extent) or switch the gates by changing the pumping strength of the reservoir. In particular, the Z gate is realised when $P = 0$ (still in the regime $J_{11} \gg E_1$) whereas the X and Y gates are realised by having real P and imaginary $P = |P| \exp(\pm i\pi/2)$, respectively. We note again that all the gates are achieved at $J_{11}\tau/\hbar = \pi + 2\pi n$.

Two-qubit gates (via direct interactions)

The setup:— Each qubit has an onsite energy E_j , a coherent pumping P_j , and no decay. Together with a hopping interaction term, one writes the Hamiltonian as

$$H = \sum_{j=\{1,2\}} E_j \hat{a}_j^\dagger \hat{a}_j + P_j \hat{a}_j^\dagger + P_j^* \hat{a}_j + J(\hat{a}_1 \hat{a}_2^\dagger + \hat{a}_2 \hat{a}_1^\dagger). \quad (11)$$

It will be shown below that this type of system is able to implement universal two-qubit gates on its initial state. We will start by presenting the working parameters for important

gates, such as the square-root-swap (sSWAP), control-X (cNOT), control-Y (cY), control-Z (cZ), square-root-iSwap (siSWAP), and swap (SWAP). These gates are written as

$$\begin{aligned}
 & \frac{1}{2} \begin{pmatrix} 2 & 0 & 0 & 0 \\ 0 & (1+i) & (1-i) & 0 \\ 0 & (1-i) & (1+i) & 0 \\ 0 & 0 & 0 & 2 \end{pmatrix}, \begin{pmatrix} 1 & 0 & 0 & 0 \\ 0 & 1 & 0 & 0 \\ 0 & 0 & 0 & 1 \\ 0 & 0 & 1 & 0 \end{pmatrix}, \\
 & \begin{pmatrix} 1 & 0 & 0 & 0 \\ 0 & 1 & 0 & 0 \\ 0 & 0 & 0 & -i \\ 0 & 0 & i & 0 \end{pmatrix}, \begin{pmatrix} 1 & 0 & 0 & 0 \\ 0 & 1 & 0 & 0 \\ 0 & 0 & 1 & 0 \\ 0 & 0 & 0 & -1 \end{pmatrix}, \\
 & \frac{1}{\sqrt{2}} \begin{pmatrix} \sqrt{2} & 0 & 0 & 0 \\ 0 & 1 & i & 0 \\ 0 & i & 1 & 0 \\ 0 & 0 & 0 & \sqrt{2} \end{pmatrix}, \begin{pmatrix} 1 & 0 & 0 & 0 \\ 0 & 0 & 1 & 0 \\ 0 & 1 & 0 & 0 \\ 0 & 0 & 0 & 1 \end{pmatrix}, \tag{12}
 \end{aligned}$$

respectively.

Simulations:— We performed a search algorithm realising the above two-qubit gates. Our numerical results show that all these gates can be achieved with gate fidelity $\bar{F} > 0.999$, see Table III for exemplary parameters. See Fig. 5 for a comparison of the high fidelity achieved with the search method for different gates. Note that genetic algorithms have been used for realising \hat{U}_{sSWAP} , \hat{U}_{cNOT} , \hat{U}_{cY} , and \hat{U}_{cZ} . The parameters for \hat{U}_{siSWAP} and \hat{U}_{SWAP} are not sensitive to small changes and therefore we did not perform precise search algorithms.

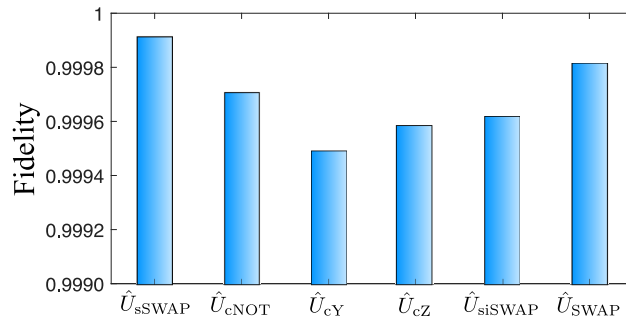


FIG. 5: Fidelity \bar{F} of various two-qubit gates for the parameters listed in Table III.

Universality:— We note that each of the two-qubit gates presented above, apart from the SWAP gate, combined with single-qubit gates form a universal set. In this way, they

TABLE III: Exemplary parameters for the realisation of two-qubit gates. We have used $\tau = E_2 t / \hbar$. All the gates are achieved with $\bar{F} > 0.999$ with $N = 10^5$. Note that the parameters for the \hat{U}_{siSWAP} and \hat{U}_{SWAP} gates are not as sensitive as the others. Especially for \hat{U}_{siSWAP} , one gets very high fidelity in the limit $E_1 = E_2 \gg P_1 = P_2, J$.

Two-qubit	Parameters				
Gates	E_1/E_2	P_1/E_2	P_2/E_2	J/E_2	τ
\hat{U}_{sSWAP}	0.923091	5.158696	5.155802	0.937275	48.168039
\hat{U}_{cNOT}	140.703597	0.958346	140.627941	2.826258	40.303524
\hat{U}_{cY}	138.217022	$-0.089054 - 0.920161i$	$0.079873 - 138.295970i$	2.881602	40.778441
\hat{U}_{cZ}	1.006724	1.094922	0.932635	117.958714	45.402586
\hat{U}_{siSWAP}	1	0.01	0.01	0.01	1181
\hat{U}_{SWAP}	1	1.5	1.5	42.8	37.6

are equivalent to each other. As an example, we recall that the cNOT gate can be created, by the cY, cZ, sSWAP or siSWAP gate with the help of single qubit gates as follows

$$\begin{aligned}
\hat{U}_{\text{cNOT}} &= [\mathbb{1} \otimes \hat{R}_z(-\pi/2)] \hat{U}_{\text{cY}} [\mathbb{1} \otimes \hat{R}_z(\pi/2)], \\
\hat{U}_{\text{cNOT}} &= [\mathbb{1} \otimes \hat{R}_y(\pi/2)] \hat{U}_{\text{cZ}} [\mathbb{1} \otimes \hat{R}_y(-\pi/2)], \\
\hat{U}_{\text{cNOT}} &= [\mathbb{1} \otimes \hat{R}_y(-\pi/2)] \hat{U}_{\text{sSWAP}} [\hat{Z} \otimes \mathbb{1}] \hat{U}_{\text{sSWAP}} \\
&\quad [\hat{R}_z(-\pi/2) \otimes \hat{R}_z(-\pi/2)] [\mathbb{1} \otimes \hat{R}_y(\pi/2)], \\
\hat{U}_{\text{cNOT}} &= [\hat{X} \otimes \hat{X}] [\hat{R}_y(-\pi/2) \otimes \mathbb{1}] \\
&\quad [\hat{R}_x(\pi/2) \otimes \hat{R}_x(-\pi/2)] \hat{U}_{\text{siSWAP}} [\hat{R}_x(\pi) \otimes \mathbb{1}] \\
&\quad \hat{U}_{\text{siSWAP}} [\hat{R}_y(\pi/2) \otimes \mathbb{1}] [\hat{Z} \otimes \mathbb{1}] [\hat{X} \otimes \hat{X}] e^{i\pi/4}.
\end{aligned} \tag{13}$$

Note that we have used the following single-qubit rotation matrices.

$$\begin{aligned}
\hat{R}_x(\alpha) &= \begin{pmatrix} \cos(\frac{\alpha}{2}) & -i \sin(\frac{\alpha}{2}) \\ -i \sin(\frac{\alpha}{2}) & \cos(\frac{\alpha}{2}) \end{pmatrix}, \quad \hat{R}_z(\delta) = \begin{pmatrix} 1 & 0 \\ 0 & e^{i\delta} \end{pmatrix}, \\
\hat{R}_y(\beta) &= \begin{pmatrix} \cos(\frac{\beta}{2}) & -\sin(\frac{\beta}{2}) \\ \sin(\frac{\beta}{2}) & \cos(\frac{\beta}{2}) \end{pmatrix}.
\end{aligned} \tag{14}$$

Even though different gates can be constructed from specific combinations of a universal set of gates, it should be noted that the ability to directly construct the gate needed for a

particular application will bring the highest efficiency in terms of operation time. Indeed the ability of the quantum reservoir neural network to learn to perform a whole range of different quantum gates is one of its advantages.

ACKNOWLEDGMENTS

SG, TK and TL were supported by the Ministry of Education (Singapore), grant no: MOE2017-T2-1-001. TP acknowledges Polish National Agency for Academic Exchange NAWA Project No. PPN/PPO/2018/1/00007/U/00001.

* Electronic address: sanjib.ghosh@ntu.edu.sg

† Electronic address: timothyliew@ntu.edu.sg

- [1] S. Webb, *Nature* **554**, 555 (2018).
- [2] D. T. Jones, *Nature Reviews Molecular Cell Biology* **20**, 659 (2019), URL <https://doi.org/10.1038/s41580-019-0176-5>.
- [3] E. J. Topol, *Nature Medicine* **25**, 44 (2019), URL <https://doi.org/10.1038/s41591-018-0300-7>.
- [4] A. Y. Hannun, P. Rajpurkar, M. Haghighpanahi, G. H. Tison, C. Bourn, M. P. Turakhia, and A. Y. Ng, *Nature Medicine* **25**, 65 (2019), URL <https://doi.org/10.1038/s41591-018-0268-3>.
- [5] A. Nagy and V. Savona, *Physical Review Letters* **122**, 250501 (2019), URL <https://link.aps.org/doi/10.1103/PhysRevLett.122.250501>.
- [6] F. Vicentini, A. Biella, N. Regnault, and C. Ciuti, *Physical Review Letters* **122**, 250503 (2019), URL <https://link.aps.org/doi/10.1103/PhysRevLett.122.250503>.
- [7] P. Mehta, M. Bukov, C.-H. Wang, A. G. R. Day, C. Richardson, C. K. Fisher, and D. J. Schwab, *Physics Reports* **810**, 1 (2019), URL <http://www.sciencedirect.com/science/article/pii/S0370157319300766>.
- [8] K. Y. M. Wong and D. Sherrington, *Physical Review E* **47**, 4465 (1993), URL <https://link.aps.org/doi/10.1103/PhysRevE.47.4465>.
- [9] N. Borodinov, S. Neumayer, S. V. Kalinin, O. S. Ovchinnikova, R. K. Vasudevan, and S. Jesse, *npj Computational Materials* **5**, 25 (2019), URL

- <https://doi.org/10.1038/s41524-019-0148-5>.
- [10] Z. Che, S. Purushotham, K. Cho, D. Sontag, and Y. Liu, *Scientific Reports* **8**, 6085 (2018), URL <https://doi.org/10.1038/s41598-018-24271-9>.
- [11] G. Ding, Y. Liu, R. Zhang, and H. L. Xin, *Scientific Reports* **9**, 12803 (2019), URL <https://doi.org/10.1038/s41598-019-49267-x>.
- [12] Y. Ming, C.-T. Lin, S. D. Bartlett, and W.-W. Zhang, *npj Computational Materials* **5**, 88 (2019), URL <https://doi.org/10.1038/s41524-019-0224-x>.
- [13] K. Roy, A. Jaiswal, and P. Panda, *Nature* **575**, 607 (2019), URL <https://doi.org/10.1038/s41586-019-1677-2>.
- [14] M. Lukoševičius, *A Practical Guide to Applying Echo State Networks*, Neural Networks: Tricks of the Trade (Springer, Berlin, Heidelberg, 2012), 2nd ed., URL https://doi.org/10.1007/978-3-642-35289-8_36.
- [15] L. Grigoryeva and J.-P. Ortega, *Neural Networks* **108**, 495 (2018), URL <http://www.sciencedirect.com/science/article/pii/S089360801830251X>.
- [16] L. F. Seoane, *Philosophical Transactions of the Royal Society B: Biological Sciences* **374**, 20180377 (2019), URL <https://doi.org/10.1098/rstb.2018.0377>.
- [17] G. Tanaka, T. Yamane, J. B. Héroux, R. Nakane, N. Kanazawa, S. Takeda, H. Numata, D. Nakano, and A. Hirose, *Neural Networks* **115**, 100 (2019), URL <http://www.sciencedirect.com/science/article/pii/S0893608019300784>.
- [18] T. Kusumoto, K. Mitarai, K. Fujii, M. Kitagawa, and M. Negoro, arXiv e-prints **arXiv:1911.12021** (2019).
- [19] D. Ballarini, A. Gianfrate, R. Panico, A. Opala, S. Ghosh, L. Dominici, V. Ardizzone, M. D. Giorgi, G. Lerario, G. Gigli, et al., arXiv e-prints **arXiv:1911.02923** (2019).
- [20] K. Fujii and K. Nakajima, *Physical Review Applied* **8**, 024030 (2017), URL <https://link.aps.org/doi/10.1103/PhysRevApplied.8.024030>.
- [21] S. Ghosh, A. Opala, M. Matuszewski, T. Paterek, and T. C. H. Liew, *npj Quantum Information* **5**, 35 (2019), URL <https://doi.org/10.1038/s41534-019-0149-8>.
- [22] M. A. Nielsen and I. Chuang, *American Journal of Physics* **70**, 558 (2002), URL <https://doi.org/10.1119/1.1463744>.
- [23] C. G. Almudever, L. Lao, X. Fu, N. Khammassi, I. Ashraf, D. Iorga, S. Varsamopoulos, C. Eichler, A. Wallraff, L. Geck, et al., in *The engineering challenges in quantum computing*

- (Design, Automation & Test in Europe Conference & Exhibition, 2017), pp. 836–845.
- [24] F. Arute, K. Arya, R. Babbush, D. Bacon, J. C. Bardin, R. Barends, R. Biswas, S. Boixo, F. G. S. L. Brandao, D. A. Buell, et al., *Nature* **574**, 505 (2019), URL <https://doi.org/10.1038/s41586-019-1666-5>.
- [25] A. Chiesa, F. Tacchino, M. Grossi, P. Santini, I. Tavernelli, D. Gerace, and S. Carretta, *Nature Physics* **15**, 455 (2019), URL <https://doi.org/10.1038/s41567-019-0437-4>.
- [26] A. G. Fowler, M. Mariantoni, J. M. Martinis, and A. N. Cleland, *Physical Review A* **86**, 032324 (2012), URL <https://link.aps.org/doi/10.1103/PhysRevA.86.032324>.
- [27] T. Esslinger, *Annual Review of Condensed Matter Physics* **1**, 129 (2010), URL <https://www.annualreviews.org/doi/abs/10.1146/annurev-conmatphys-070909-104059>.
- [28] W. Hofstetter and T. Qin, **51**, 082001 (2018), URL <http://dx.doi.org/10.1088/1361-6455/aaa31b>.
- [29] L. Tarruell and L. Sanchez-Palencia, *Comptes Rendus Physique* **19**, 365 (2018), URL <http://www.sciencedirect.com/science/article/pii/S1631070518300926>.
- [30] I. Carusotto, D. Gerace, H. E. Tureci, S. De Liberato, C. Ciuti, and A. Imamoglu, *Physical Review Letters* **103**, 033601 (2009), URL <https://link.aps.org/doi/10.1103/PhysRevLett.103.033601>.
- [31] C. E. Bardyn and A. Imamoglu, *Physical Review Letters* **109**, 253606 (2012), URL <https://link.aps.org/doi/10.1103/PhysRevLett.109.253606>.
- [32] D. E. Chang, V. Vuletić, and M. D. Lukin, *Nature Photonics* **8**, 685 (2014), URL <https://doi.org/10.1038/nphoton.2014.192>.
- [33] D. G. Angelakis, *Quantum Simulations with Photons and Polaritons: Merging Quantum Optics with Condensed Matter Physics* (Springer International Publishing, Cham, Switzerland, 2017).
- [34] C. Vaneph, A. Morvan, G. Aiello, M. Féchant, M. Aprili, J. Gabelli, and J. Estève, *Physical Review Letters* **121**, 043602 (2018), URL <https://link.aps.org/doi/10.1103/PhysRevLett.121.043602>.
- [35] A. Delteil, T. Fink, A. Schade, S. Höfling, C. Schneider, and A. Imamoglu, *Nature Materials* **18**, 219 (2019), URL <https://doi.org/10.1038/s41563-019-0282-y>.
- [36] R. P. A. Emmanuele, M. Sich, O. Kyriienko, V. Shahnazaryan, F. Withers, A. Catanzaro, P. M. Walker, F. A. Benimetskiy, M. S. Skolnick, A. I. Tartakovskii, et al., arXiv:1910.14636 (2019).

- [37] O. Kyriienko, D. N. Krizhanovskii, and I. A. Shelykh, arXiv:1910.11294 (2019).
- [38] T. Pierre, L. J. Hanna, S. S. F., H. H. R., G. Stephan, S. Vahid, L. Peter, and R. Nir, *Nanophotonics* **8**, 1641 (2019), URL <https://www.degruyter.com/view/j/nanoph.2019.8.issue-10/nanoph-2019-0126/nanoph-2019-0126.x>
- [39] D. Roy, C. M. Wilson, and O. Firstenberg, *Reviews of Modern Physics* **89**, 021001 (2017), URL <https://link.aps.org/doi/10.1103/RevModPhys.89.021001>.
- [40] M. Fitzpatrick, N. M. Sundaresan, A. C. Y. Li, J. Koch, and A. A. Houck, *Physical Review X* **7**, 011016 (2017), URL <https://link.aps.org/doi/10.1103/PhysRevX.7.011016>.
- [41] F. Nissen, S. Schmidt, M. Biondi, G. Blatter, H. E. Türeci, and J. Keeling, *Physical Review Letters* **108**, 233603 (2012), URL <https://link.aps.org/doi/10.1103/PhysRevLett.108.233603>.
- [42] H. J. Snijders, J. A. Frey, J. Norman, H. Flayac, V. Savona, A. C. Gossard, J. E. Bowers, M. P. van Exter, D. Bouwmeester, and W. Löffler, *Phys. Rev. Lett.* **121**, 043601 (2018), URL <https://link.aps.org/doi/10.1103/PhysRevLett.121.043601>.
- [43] P. Scarlino, D. J. van Woerkom, U. C. Mendes, J. V. Koski, A. J. Landig, C. K. Andersen, S. Gasparinetti, C. Reichl, W. Wegscheider, K. Ensslin, et al., *Nature Communications* **10**, 3011 (2019), URL <https://doi.org/10.1038/s41467-019-10798-6>.
- [44] J. Biamonte, P. Wittek, N. Pancotti, P. Rebentrost, N. Wiebe, and S. Lloyd, *Nature* **549**, 195 (2017), URL <https://doi.org/10.1038/nature23474>.
- [45] A. Kutvonen, T. Sagawa, and K. Fujii, arXiv e-prints **arXiv:1807.03947** (2018).
- [46] E. Farhi and H. Neven, *Classification with quantum neural networks on near term processors* (2018), URL <https://ui.adsabs.harvard.edu/#abs/2018arXiv180206002F>.
- [47] E. Grant, M. Benedetti, S. Cao, A. Hallam, J. Lockhart, V. Stojevic, A. G. Green, and S. Severini, *npj Quantum Information* **4**, 65 (2018), URL <https://doi.org/10.1038/s41534-018-0116-9>.
- [48] I. Cong, S. Choi, and M. D. Lukin, *Nature Physics* **15**, 1273 (2019), URL <https://doi.org/10.1038/s41567-019-0648-8>.
- [49] V. Havlíček, A. D. Córcoles, K. Temme, A. W. Harrow, A. Kandala, J. M. Chow, and J. M. Gambetta, *Nature* **567**, 209 (2019), URL <https://doi.org/10.1038/s41586-019-0980-2>.
- [50] M. H. Amin, E. Andriyash, J. Rolfe, B. Kulchytskyy, and R. Melko, *Physical Review X* **8**, 021050 (2018), URL <https://link.aps.org/doi/10.1103/PhysRevX.8.021050>.

- [51] L. Banchi, N. Pancotti, and S. Bose, *npj Quantum Information* **2**, 16019 (2016), URL <https://doi.org/10.1038/npjqi.2016.19>.
- [52] E. Zahedinejad, J. Ghosh, and B. C. Sanders, *Physical Review Applied* **6**, 054005 (2016), URL <https://link.aps.org/doi/10.1103/PhysRevApplied.6.054005>.
- [53] X. Yang, J. Li, and X. Peng, *Science Bulletin* **64**, 1402 (2019), URL <http://www.sciencedirect.com/science/article/pii/S2095927319304104>.